⊙ Technical Paper

Application of Fracture Mechanics Method to Offshore Structural Crack Instability Analysis

H.C. Rhee* and M.M. Salama**

해양구조물의 균열불안정성 해석에 대한 파괴역학의 응용

李 喜 鍾·M.M. 샐러머

Key words : Crack Instability Analysis(균열불안정성 해석), Fracture Mechanics Method(파괴역학적 방법), J-Integral(J-적분), COD Design Curve Method(COD 설계곡선법), Failure Assessment Diagram(파괴평가도)

초 록

균열불안정 해석법인 COD설계곡선법과 R6파괴 평가도법에 있어서 그 응용 한계의 확립과 타당성 수준의 정량화를 위해 포괄적인 비교 연구가 수행되었다. 참고로서 J-적분 균열불안정성 해석법이 이용되었다.

본 연구의 결과로서, 균열확장의 유무에 대한 R6 파괴 평가도법이 매우 우수한 방법임을 보여준다. COD설계곡선법에 대한 영국 표준국 순서에 따른 결과로서는, 큰 스캐터 밴드를 가진 상당량의 부당성해를 보여준다. 이러한 COD설계곡선법의 해를 개선하기 위한 새로운 접근법이 개발되었고, 그 타당성이 입증되었다.

1. Introduction

Fracture mechanics methods are becoming an important tool to perform an engineering critical assessment (ECA) of defects in offshore structures. The main objective of the ECA analysis is to establish the maximum tolerable defect size which would not compromise the service requirment. This can be achieved by ensuring that the fatigue life of joints with defects is greater than the required service life and that any defect does not attain a size to cause either crack instability or plastic collapse.

There are several fracture mechanics methods that have been proposed to establish conditions of crack instability. These methods are the crack opening displacement(COD), failure assessment diagram (R6), and J-integral crack instability procedures. The COD method is the one that is extensively used by the offshore industry.

In a previous paper by the authors,[1] comparison between the three methods were performed to establish the limits of applicability and quantify the levels of conservatism in both the COD and R6 methods. The paper reported several cases where apparent lack of conservatism was observed in the COD results. This paper presents an extension of the previous study by extensive analysis of different load cases. Analysis of som these cases was only possible by the resent publication of their

* Member, Conoco Inc., U.S.A.
** Conoco Inc., U.S.A.

J-integral solution.[2] Also, a recently developed R6 curve for hardening materials that were made available to the authors allowed the extension of the previous R6 solutions. The paper also developed several modifications to the current COD analysis approach to ensure its reliability for ECA analysis. In this study, the J-integral results were used as reference because, as was discussed in the previous work, it represents the one with the most rigorous analysis procedures.

2. Geometry and Material

For fair comparison between the three considered fracture mechanics methods, only flaw geometries that have known J-integral solutions, plastic collapse loads, and stress intensity factor solutions were selected. Also, consistency was maintained among the used material properties for all the analysed cases. The material properties were selected from a data base[3,4] created for ductile tearing instability studies for A508 Class A steel, which has similar charactristics structural steels.

2.1 Geometry

Figure 1 presents the geometries and loading conditions considered. To study the geometry effects on the solutions, the center-cracked tension panel (CCT), the single-edge notched panel, and the pipe with an internal circumferential flaw (PIPE) were selected. To consider the loading mode effects, the single-edge notched panel was loaded with three-point bending (SENB), which represents a pure bending load, pure tension (SENT), and combined tension and bending. For the combined tension and bending load, tow cases were investigated-i.e., one with $\lambda=8/1$ (SENM8) and the other with $\lambda=-1/16$ (SENM 16), where λ is the ratio between the applied moment normalized by the specimen width and the applied tensile load, viz., $\lambda=M/(Pb)$.

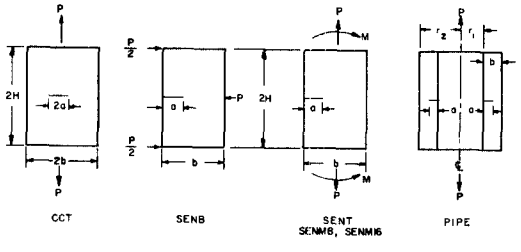

Fig. 1 Structural geometry and load

For all geometries, three different widths were considered. They $b=10(254)$, 20(508), and 30(762) inches(mm). The H/b ratios are 3(CCT), 2(SENB), and 1(SET and SENT). For all geometries, the cases where crack depth was half of the width were analyzed. For the width, $b=20(254)$ inches (mm), the cases with the ratios $a/b=1/8$ and 1/4 were also considered. For the pipe, the ratio rl/b was maintained equal to 5. The widths of the geometries were selected to ensure that plastic collapse does not proceed crack instability to avoid the cases where the COD design curve method is not valid.

The stress intensity factor for the structures can be given as :

$$K_I=\sigma F\sqrt{\pi a} \tag{1}$$

where σ is the applied stress and F is the structural configuration factor (see Table 1)5.

In the present analyses, the deformation plasticity J-integral solution[2,6] was used for all considered geometries. The solution is, in general, given as :

$$J=\frac{K_I(a_e)^2}{E'}+\alpha\sigma_y c_y\, f(a,b)\, h(n,a/b)\left(\frac{P}{P_0}\right)^{n+1} \tag{2}$$

where K_I(ae) is the stress intensity factor solution with plastically adjusted crack depth, ae (see Reference 6 for its expression) ; $E'=E$ for a plane stress state ; and $E'=E/(1-\nu^2)$ for a plane strain state, with E and ν being Young's modulus and Poisson's ratio, respectively ; f(a, b) is d(b-a) for SENB and a(b-a)/b for the other geometries ; h(n, a/b) is a function of n and a/b ratio ; P is the applied load ; P_0 is the plastic collapse load of lhe geometry of a perfectly plastic material with the yield stress σy ; and α and n are Ramberg-Osgood uniaxial stress-strain curve parameters defined as:

$$\frac{e}{e_y}=\frac{\sigma}{\sigma_y}+\alpha\left(\frac{\sigma}{\sigma_y}\right)^n \tag{3}$$

The plastic collapse loads obtained from the elastic-

Table 1 Problem definition

Geometry	Stress state (Plane)	Symbol (Figs. 6-14)	F	P_0
CCT	strain	□	$\left[1-0.25\left(\frac{a}{b}\right)^2+0.06\left(\frac{a}{b}\right)^4\right]\sqrt{sec\frac{\pi a}{2b}}$	$4(b-a)\sigma_y/\sqrt{3}$
	stress	■		$2(b-a)\sigma_y$
PIPE	—	○	See Reference 6	$\frac{2[r2^2-(r_1+a)^2]\,\sigma_y}{\sqrt{3}\,(r_2^2-r_1^2)}$
SENT	strain	△	$F=F_1=A(0.752+2.02\frac{a}{b}+0.37B^3)$	$1.455C(b-a)\sigma_y$
	stress	▲		$1.072C(b-a)\sigma_y$
SENM8	strain	+	$\frac{F_1+6\lambda A(0.92_5+0.199B^3)}{1+6\lambda}$	$\frac{2\sigma_y b}{\sqrt{3}}\left[-D+\sqrt{D^2+\left(\frac{b-a}{b}\right)^2}\right]$
SENM16	strain	*		
SENM16	strain	◇	$1.07-1.735\left(\frac{a}{b}\right)+8.2\left(\frac{a}{b}\right)^2$	$0.728\sigma_y(b-a)^2/H$
	strain	◆	$-14.18\left(\frac{a}{b}\right)^3+14.57\left(\frac{a}{b}\right)^4$	$0.536\sigma_y(b-a)^2/H$

σ_y is the material yield strength, $\lambda=\frac{M}{Pb}$

$A=\sqrt{\frac{2b}{\sigma a}tan\frac{\pi v}{2b}}\,sec\left(\frac{\pi a}{2b}\right)$ $B=1+sin\left(\frac{\pi a}{2b}\right)$ $C=1+\left(\frac{a}{b-a}\right)^2-\left(\frac{a}{b-a}\right)$, $D=\left|2\lambda+\frac{a}{b}\right|$

plastic fracture handbooks[2,6] are listed in Table 1. The appropriate h functions with n=7 of References 2 and 6 were used for the problems analyzed.

2.2 Material Property Data

The material properties required for the present study are given in Table 2 and Figure 2. The COD resistance curve, from which the critical COD, δc, was obtained, and the J_R curve were calculated from the load-load point displacement record of a 10T compact tension specimen(with 20-inch width and about a 10-inch original crack depth) using the unloading compliance method.[7] The J-integral values along The J_R curve were calculated by the moving crack correction method.[8] For the COD value computation, a procedure simi-

Table 2 Mechanical properties

Young's moduls, E, *ksi(MPa)* :	30,000(207,000)
Yield strength, σ_y, *ksi(MPa)* :	53.14(366.4)
Ultimate strength, σ_u, *ksi(MPa)* :	80.8(557.12)
Poisson's ratio :	0.30
J_{IC}, *ksi·in(MPa·mm)* :	1.2(210.12)
COD value, δ_c, *in (mm)* :	0.0365(0.927)
Remberge-Osgood coeffients : α :	1.346
n :	7.0

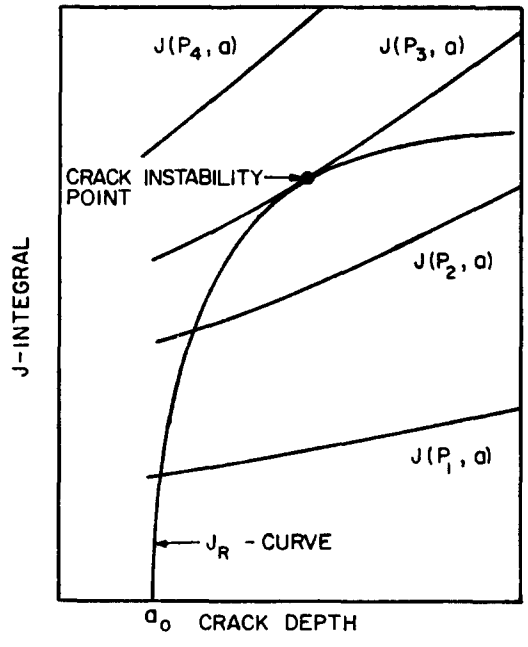

Fig. 2 The R-curve concept using J-integral

lar to the tentative ASTM standard method[3] was used. The critical COD value, δc, was sampled at the maximum load point along the COD resistance curve. Therefore, the critical COD value used in the analyses is corresponding to δm[9].

3. Analysis Procedure

3.1 J_R Crack Instability Analysis Method

The J-integral method is an extension of the classical R-curve method to elastic-plastic regime based on the J-integral concept.[10] The concept of the method is graphically represented in Figure 3. The crack instability point is reached when the following two conditions are met:

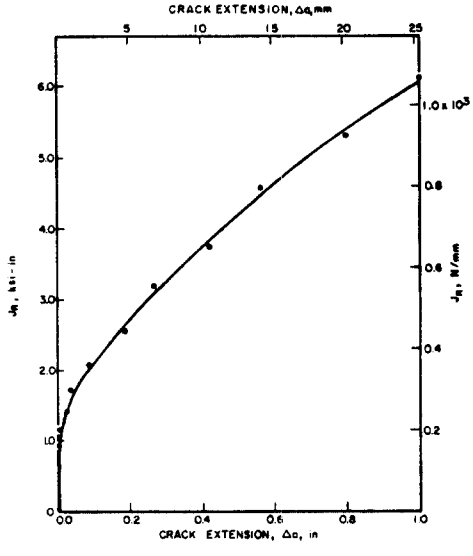

Fig. 3 J_R-curve of an A508 Class A steel

$$J(P, a) = J_R(a) \tag{4}$$

$$\frac{dJ}{da} = \frac{dJ_R}{da} \tag{5}$$

where P is the applied load ; $J(P, a)$ is the applied J-integral ; and J_R(a) is the material crack growth resistance expressed in terms of J-integral. In solving the above system of equations, the critical load assessment method (CLAM)[11] was used because of its simplicity.

To solve the system of Equations 4 and 5 the CLAM develops the relationship between J and P, subject to the crack equilibrium condition during stable crack growth. Since one-to-one correspondence between P and J exists during stable crack growth from Equation 4, it can be shown that :

$$\frac{dP}{dJ} = \left(\frac{dJ_R}{da}\right)^{-1}\left(\frac{dJ_R}{da} - \frac{\partial J}{da}\right) \tag{6}$$

Equation 6 implies that if dP/dJ vanishes along the above J-P relationship, Equation 5 with constant P will be satisfied. Since this J-P relationship was developed based on Equation 4, the condition $dP/dJ = 0$ is sufficient to satisfy the system of Equations 4 and 5. Thus the critical load is the value of P which makes the slope of the above J-P curve vanish (Figure 4). The CLAM eliminates the need for the evaluation of tearing modulii in a crack instability analysis.

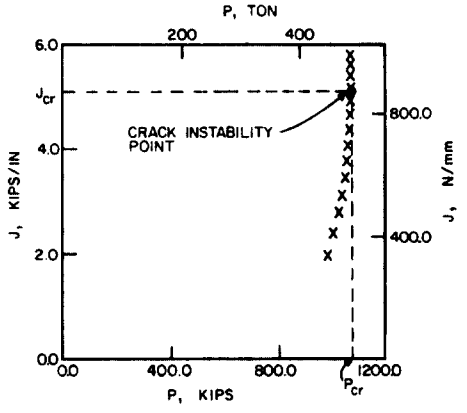

Fig. 4 Critical load assessment method for crack instability analysis

In most the analyzed cases, the J-controlled crack growth Conditions 12 are considered to be satisfied, since the J_R curve used in the analyses was developed through a very conservative test specimen (10T CT), and the crack extension before crack instability was small compared to the thickness and uncracked ligament length (typically around 6 or to 7 percent), excluding some small exceptions. Based on our previous experiences[13] for cases such as these, the conditions for J-controlled crack growth are believed to be satisfied.

3.2 R6 Failure Assessement Diagram Method

The $R6$ failure assessment diagram method was developed based on the postulation tha failure was bounded by brittle fracture at one extreme and by plastic collapse at the other. The formula interpolating between these two limits was derived using the plane strain COD expression of Dugdale strip

yield model[14]:

$$K_r = S_r\left[\frac{8}{\pi^2}\ln\ sec\left(\frac{\pi}{2}S_r\right)\right]^{-1/2} \quad (7)$$

where K_r is the ratio between the elastic stress intensity factor and the corresponding fracture toughness, $K_I(a)$ $\sqrt{J_R E'}$, and S_r is the ratio between the applied load, P/P_0. Equation 7 is generally presented by a diagram in an $S_r - K_r$ plane, as shown in Figure 5. The analysis procedures are provided in Reference 14. For a given structure of a known defect size and subjected to a specified load, if the structural assessment point (S_r, K_r) falls within the envelope of Equation 7, as shown by Point A in Figure 5, failure will not occur. The critical failure load for the geometry is the magnitude P that makes the assessment point coincide with Equation 7 as Point A' of Figure 5.

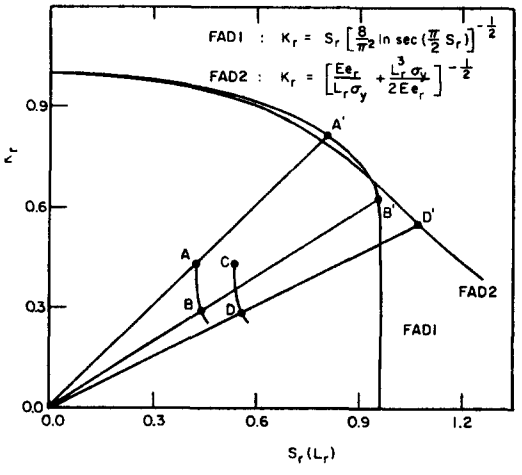

Fig. 5 R6 failure assessment diagram method

The assessment Point A' (FAD) is based on K_r, which was calculated with the initiation fracture toughness, JIC. Thus the resulting critical load represents the crack initiation point. To include stable tearing in the critical load calculation(FAD1), the locus Curve A-B of Figure 5) determined by the $S_r - K_r$ pairs based on the J_r curve should be developed. The critical point, B'(Figure 5), is the point at which the locus meets tangentially with Equation 7, when it is radially translated.

While the structural characteristics, such as geometry, loading conditions, and material properties of a problem, can be correctly reflected in the determination of the assessment point, A, the method does not fully consider them in the determination of the critical state represented by Equation 7. It is postulated that Equation 7 can provide conservative results for all practical structures. Miline[15] recently developed a new failure assessment curve for hardening materials (Figure 5). For the new curve(FAD2), Sr parameters should be replaced by $L_r = S_r(\sigma_y + \sigma_u)/(2\sigma)$, and the remaining procedures are identical to those of FAD1 (Curve C-D of Figure 5). In FAD2, er is a strain parameter, which is obtaind by submitting $L_r\sigma y$ for the stress in the material uniaxial stress-strain relationship. In addition to reflecting material's hardening behavior, the new curve is supposed to be intensitive to the charactristics of a specific geometry.

3.3 The COD Design Curve Method

As a condition for safety of a flawed structure, the COD design curve provides a relationship among the material fracture thoughness in terms of the crack opening displacement (δ_c), the allowable crack size given in terms of the equivalent semicrack depth in an infinite plate ($\bar{a}$), applied loads in terms of strain (e) or stresses (σ), and other matrial properties, such as yield strain (e_y) and yield stress(σ_y). This relationship, which, originating from the plane stress relationship between COD and e/e_y of strip yield model, is semiempirical. can be given as :

$$\frac{\delta_c}{2\pi\ ey^a} = \left(\frac{e}{e_y}\right)^2 \text{for } \frac{e}{e_y} \leq 0.5 \quad (8a)$$

$$= \frac{e}{e_y} - 0.25 \text{ for} \frac{e}{e_y} \leq 0.5 \quad (8b)$$

The relationship between $\bar{a}$ and the crack depth of a specific geometry is established through the proper stress intensity factor solutions as :

$$K_I = \sigma\sqrt{\pi\bar{a}} = \sigma F\sqrt{\pi a} \quad (9a)$$

or

$$\bar{v} = F^2 a \quad (9a)$$

The implemetation of this method can be achieved through the guidance of the British Standards Ins-

titute Published Document PD6493.[16] In this document, the srain ratio (e/e_y) can be replaced by the corresponding stress ratio (σ/σ_y) as long as e/e_y is less than 2. The applied stress, σ, is the combination of the respective membrane and banding stresses. The relationship between a and $\bar{a}$ is determined graphically for both surface and embedded flaws from graphs which were developed basically from the stress intensity factor solution data for tensile loading problems.

In the PD 6493 procedures, BOD(PD), the structural characteristics are not explicitly reflected in an analysis, as can be seen in Equation 8. They are considered only through the $\bar{a}$ calculation (Equation 9). However, the effects of loading mode are still ignored in Equation 9. Thus, if the magnitude of the applied stress, σ, and the a/b ratio are identical, the resulting COD(PD) solutions are the same regardless of the problem geometry (SENB, SENM, SENT, or PIPE).

Since the previous study I demonstrated that the COD(PD) solutions can be unconservative for a certain class of problems, in the present study, we have attempted to improve the solution quality without altering the COD design curve itself. The solution quality was improved by using the F function of Table 1, corresponding to specific geometry and loading conditions, for the $\bar{a}$ calculation and using the deformation plasticity stress-strain relationship (Equation 3) in a plane stress state for the calculation of σ/λ_y from e/e_y. The resulting COD(DPA) solutions behaved much better than those COD(PD). Although these two added features dramatically improved the COD predictions, a few unconservative solutions were newly developed. It can also be contented that the weakening effects of plastic yielding on a flawed geometry should be included in the $\bar{a}$ calculation. In this case, the F function should be based on the $\bar{a}$ calculation. In this case, the F function should be based on the plastically adjusted crack depth ae, rather than a, in the $\bar{a}$ calculation. The resulting COD(DPA, PCA) solution procedures eliminated the unconservative solutions from the COD(DPA) procedures, as can be seen later.

4. Results and Discussion

A comparison was performed between the critical stresses normalized by the material yield strength obtained by the CLAM and by both the failure assessment diagram, FAD (Figures 6 through 8), and the COD design curve method, COD (Figures 9 through 11). The symbols respresenting the solutions obtained by different methods are presented in Table 1. Though the problem geometries were selected so that plastic collapse will not proceed crack instability, as stated earlier, five out of the considered forty-five cases developed the critical stress levels (CLAM) higher than the respective plastic collapse loads on the formulas in Table 1. In the calculation of the plastic collapse load, the flow stress as defined by the average of the yield and ultimate strengths was used to account for the material hardening behavior instead of the yield strength. These solutions were included in comparison, since they are not significant in number.

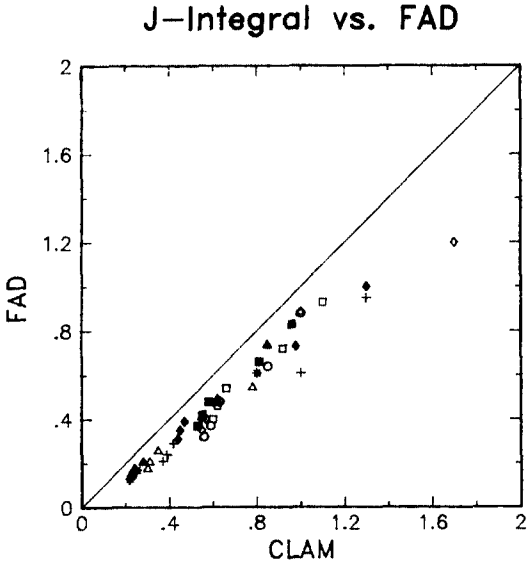

Fig. 6 Comparison of critical stress normalized by material yield strength(CLAM vs.FAD)

Generally, all the FAD relations behave well with narrow scatter bands with comparatively uniform levels of safety margin throughout the critical load levels. All but one FAD1 solution (i.e., plane strain in SENT with $b=20$ (508) inches (mm) and $a/b=$.

1/8) are conservative (Figure 7). Figure 4 and 5 are the graphical presentation of the CLAM and FAD solutions, respectively, of this problem.

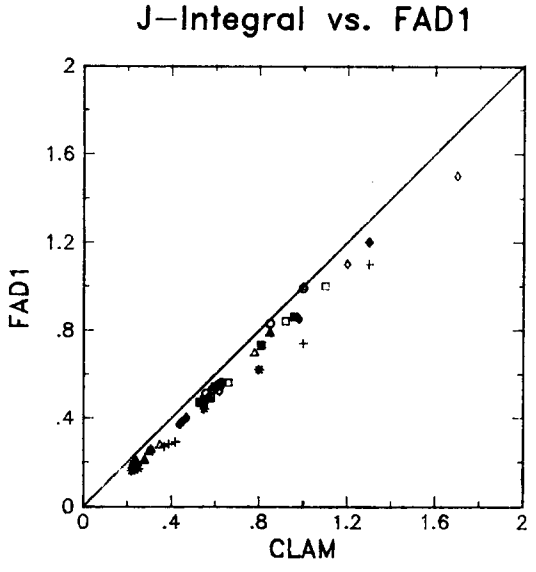

Fig. 7 Comparison of critical stress normalized by material yield strength (CLAM vs. FAD1)

It is apparent, from Figures 6 though 8, that the size of the data scatter of the solution groups with crack extension (FAD 1 and FAD2) is smaller than that with ignoring crack extension(FAD). It is clear that incorporating stable tearing before crack instability to the solution procedure improved the solution quality (reduced the scatter band) in the *R6* failure assessment method, as can be observed from a comparison between the FAD1 and FAD solutions. Since the magnitude of stable tearing depends on the structural characteristics of a problem, this solution quality improvement by including crack extention is consistant with the analysis system. The magnitudes of the safety margins of these solution groups are roughly in ascending order of FAD1, FAD2, and FAD. The FAD solutions are bound to be more conservative than the FAD1 solutions since crack etension was ignored in the FAD solutions.

The most desirable feature of the R6 solutions is their predictability as critical load parameters, as demonstrated by the narrow scatter band. Based on the results presented here, the method appears to be reliable for general application, utilizing a safety factor concept and engineering judgement.

The assertion[15] that FAD2 is insensitive to structural geometry has been demonstrated in Figure 8. However, so is FAD1 (Figure 7), which is based-on the strip yield model. It could be the two-parameter concept (K_r, S_r) that makes the R6 solution behave isensitively to structural geometry when it is applied with a plausible failure assessment curve. Thus the most significant challenge for the R6 method, as a tool for the evaluation of criticality condition, is the quantification of the level of conservatism, since its applicability limit can be well defined through data similar to what are presented by this work.

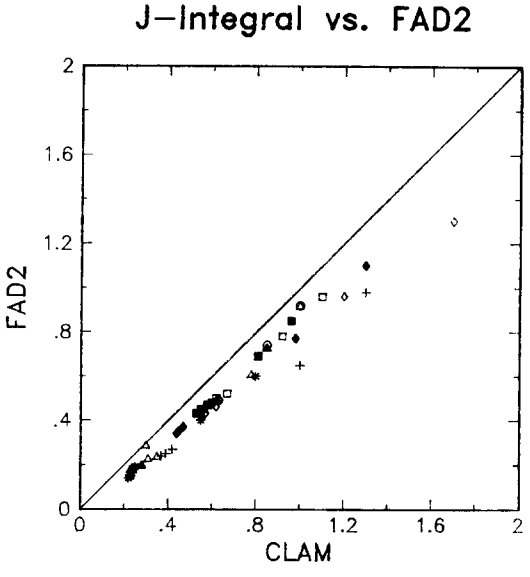

Fig. 8 Comparison of critical stress normalized by material yield strength (CLAM vs.FAD2)

Figures 9 through 11 give the comparison between the CLAM and COD solutions. It is apparent from Figure 9 that scatter band of the COD(PD) solution is larger for the bending load cases than for the pure tensile load problems. The unconservative solutions start to appear when the calculated critical load level exceeds 60 percent of the material yield strength. This solution unconservativeness seems to be more closely related to the stress

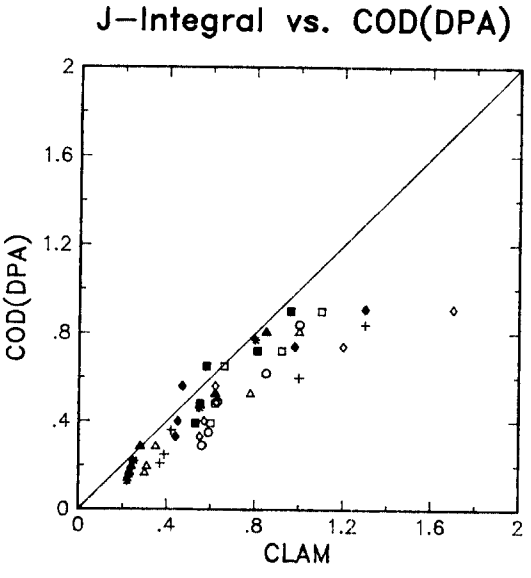

Fig. 9 Comparison of critical stress normalized by materia yield strength CLAM vs.COD (PA)

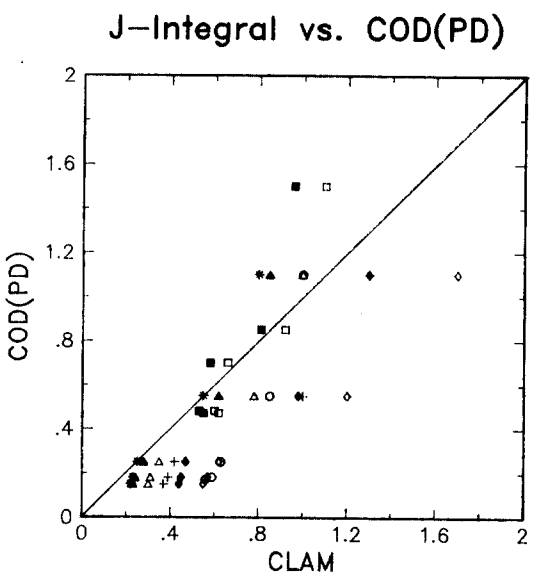

Fig. 10 Comparison of critical stress normalized by material yield strength CLAM vs. COD (PA)

level than the geometric and the loading configurations of a problem. Since the PIPE solution falls on the boundaries of the solution scatter band, it could mean that the COD(PD) solution is sensitive to the geometric characteristics of a problem.

The COD solutions were greatly improved in quality when the structural characteristics were considered in the conversion between $\bar{a}$ and a ; and the actual stress-strain relationship was used in the conversion between e/e_y and σ/σ_y (Equation 8) by using the deformation plasticity stess strain relationship. The improvement in solution scatter is mainly the result of using the stress intensity factor solution of the actual geometry in the $\bar{a}$ calculation (Equation 9). However, three of the COD (DPA) solutions (CCT, SENT and SENB) of plane stress states newly became unconservative(Figure 9). As can be seen from Figure 10, the COD solutien can be further improved by using the plastically adjusted crack depth in the $\bar{a}$ calculation. The resulting COD(DPA, PCA) solution procedure eliminated all unconservative solutions from the COD design curve analyses, and the solution scatter band of this procedure is the smallest among all three groups of the COD solutions.

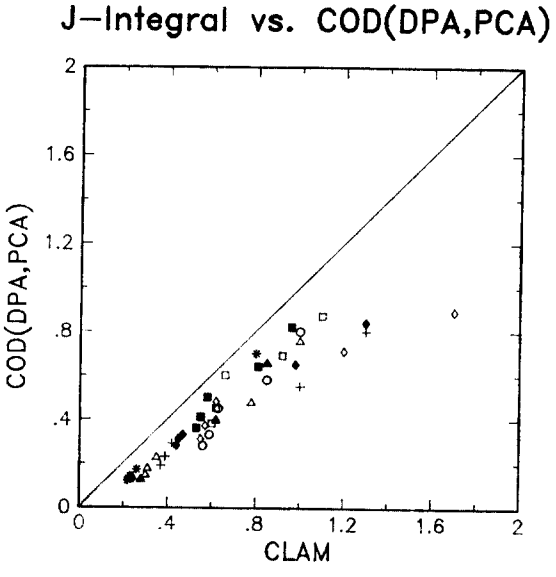

Fig. 11 Comparison of critical stress normalized by material yield strength CLAM vs. COD (DPA, PCA)

The elimination of the unconservative solution is the most significant for the reliability of the COD design curve method. It is so because the COD design curve method is considered to have a built-in safety factor[9] (vaguely defined as 2.0) and its sol-

ution is used as an allowable design parameter rather than a critical value.

In addition to the unconservativeness of the solutions, which are defined as acceptable design parameters, the unpredictable nature (large soution data scatter) of the COD(PD) solutions makes the COD design curve method unreliable. Even though a method develops some unconservative solutions as in FAD1 and COD(DPA), if the solution trend is predictable (narrow solution data scatter) as in FAD1 and the trend can be generalized, such a method can be used as a reliable engineering tool. Therefore, the COD(DPA, PCA) procedure may be able to provide a means to resolve most of the difficulties involved in the original COD design curve method, COD(PD).

5. Conclusions

Rigorous comparisons of crack instability solutions were perfomed for various flaw geometries under different loading conditions, obtained by the J-integral, the COD design curve, and the R6 failure assessment conclusions can be obtained :

1) The R6 failure assessment method developed well-behaving solutions with and without consideing crack extension in the analyses.
2) When crack extension was also reduced compared to that obtained without crack extension.
3) The British Standard Institution's published document procedures for the implementation of the COD design curve method can result in unconservative solutions for a certain class of problems, especially for cases with high levels of applied stresses. For these solution procedures, the effects of the loading mode and the geometric characteristics of a problem on the solutions seem to be significant.
4) It has been demonstrated that the COD design curve method solutions can be improved by using an actual stress-strain relationship in calculating the load parameter and using the actual stress intensity factor solution in the calculation of flaw depth parameter. The solution can be improved further by using a plastically adjusted crack depth for the calculation of the flaw depth parameter. These series of simple modification can make the original COD design curve method a reliable design analysis tool.
5) To obtain reliable results by using the COD design curve method, one should understand the system thoroughly and sound engineering judgment.
6) To generalize the results of the present study, it is necessary to expand the data base created by this study through more analyses and experimental verification.

6. Acknowledgments

The authors are grateful to the management of Conoc Inc. for permission to publish this paper. It is acknowledged that Dr. Miline of CEGB, Leatherhead, provided the materials for the FAD1 and FAD2 curves.

References

1) Rhee, H.C., and M.M. Salama, "Comparative Evaluation of Fracture Mechanics Methodologies as Applied to Offshore Structural Design and Integrity Analyses," OTC 4772, Offshore Technology Conference, Houston, Texas, 1984
2) G.E.C., "Advances in Elastic-Plastic Fracture Analysis," EPRI NP-3607, General Electric Company, August 1984
3) Landes, J.D., D.E. McCabe, H.A. Ernst, W.H. Pryle, and P.K. Liaw, "Elastic-Plastic Methology to Establish R-Curves and Instability Criteria," Sixth Semiannual Report, EPRI RP-1238-2, August 1982
4) Landes, J.D., and D.E. McCabe, "Elastic-Plastic Methodlogy to Establish R-Curves and Instability Criteria Topical Report" : Complication Data, EPRI RP-1238-2, December 1981
5) Tada, H., P.C. Paris, and G.R. Irwin, "The Stress Analysis of Cracks", Handbook, Del Research Corporation, Hellertown, Pensylvania, 1973

6) G.E.C., "An Engineering Approach for Elastic-Plastic Fracture Analysis," EPRI RP-1237-1, General Electric Company, July 1981
7) Clarke, W.R., W.R. Andrews, P.C. Paris, and D.W. Schmidt, "Single Specimen Tests for JIC Determination," ASTM STP590, American Society for Testing and Materials, 1976
8) Ernst, H.A., P.C. Paris, and J.D. Landes, "Estimations on J-Integral and tearing Modulus T, From a Single Specimen Test," ASTM STP743 on 13th National Symposium, November 1981
9) Dawes, M.G., and M.S. Kamatch, "The Crack Opening Displacement (COD) Design Curve Approach to Crack Tolerance", Conf. on the Significance of Flaws in Pressurized Components, Institution of Mechanical Engineers, London, England, May 1978
10) Rice, J.R., "A Path Independent Integral and the Appropriate Analysis of Strain Concentration by Notches and Cracks", J. Appl. Mech., 34, 1967
11) Rhee, H.C., "Critical Load Assessment Method for Stable Crack Growth Analysis", ASTM STP868, 16 th Symposium on Fracture Mechanics, American Society of Testing and Materials, Columbus, Ohio, August 1983
12) Hutchinson, J.W., and P.C. Paris, "Stability Analysis of J-Controlled Crack Growth", Elastic-Plastic Fracture, ASTEM STP688, J.D. Lands, J.A. Begley, and F.A. CrackeEds, 1979
13) Rhee, H.C., and K,K. Yoon, "Application of the Tearing Instability Theory to Elastic-Plastic Fracture Analysis", Presented at the ASME Annual Winter Meeting, Phoenix, Arizona, 1982
14) Harrison, R.P., K. Loosemore, and J. Milne, "Assessment of the Integrity of Structures Containing Defects", CEGB Report No. R/H/R6, Central Electricity Generating Board, UK, 1976
15) Milne, J., CEGB, Leatherhead, UK, Private Communication, December 1984
16) B.S.I., "Guidance on Some Methods for the Derivation of Acceptance Levels for Defects in Fusion Weld Joints," British Standard Institution, PD6493 1980

◇